CONFLUENTES MATHEMATICI

Serge NICAISE and Fatiha BEKKOUCHE

A posteriori error estimates for a fully discrete approximation of Sobolev equations

Tome 11, n° 1 (2019), p. 3-28.

<http://cml.cedram.org/item?id=CML_2019__11_1_3_0>

Confluentes Math.
11, 1 (2019) 3-28

A POSTERIORI ERROR ESTIMATES FOR A FULLY DISCRETE APPROXIMATION OF SOBOLEV EQUATIONS

SERGE NICAISE AND FATIHA BEKKOUCHE

Abstract. The paper presents an a posteriori error estimator for a (piecewise linear) conforming finite element approximation of some (linear) Sobolev equations in $\mathbb{R}^d$, $d = 2$ or 3, using implicit Euler's scheme. For this discretization, we derive a residual indicator, which uses a spatial residual indicator based on the jumps of conormal derivatives of the approximations and a time residual indicator based on the jump (in an appropriated norm) of the successive solutions at each time step. Lower and upper bounds are obtained with minimal assumptions on the meshes. Numerical experiments that confirm and illustrate the theoretical results are given.

1. Introduction

This paper deals with the a posteriori analysis of linear Sobolev equations of type

$$L_1 u_t + L_2 u = f \quad \text{in } \Omega \times (0,T),$$

where L_1, L_2 are second order differential operators, approximated using implicit Euler's scheme in time and a (piecewise linear) conforming finite element approximation in space. Such problems are interesting not only because they are generalizations of a standard parabolic problem but also because they arise naturally in a large variety of applications (model of fluid flow in fissured porous media [2], two-phase flow in porous media with dynamical capillary pressure [12, 14], heat conduction in two-temperature systems [8, 25] and shear in second order fluids [11, 24]).

Several approaches have been introduced to define error estimators for parabolic problems (like the heat equation, corresponding to the case where L_1 is reduced to the identity operator), let us quote [4, 5, 6, 7, 15, 18, 21, 22, 27, 28, 29]. To be able to extend these techniques to Sobolev equations, we need to be able to manage the replacement of the identity operator by a second order elliptic one. To the best of our knowledge such an approach has not been considered. Indeed we only found two papers related to this topic. The first one [17] highlights a superconvergence phenomena on cartesian grids whose estimates can be bounded by the norms of known data so that some useful a posteriori error estimates can be derived, while the second one [26] obtains some error estimates by solving local nonlinear or linear pseudo-parabolic equations for corrections to the solution.

The schedule of the paper is the following one: Section 2 recalls the continuous problem and its discretizations. In Section 3 we introduce some notations and give some useful properties. Section 4 is devoted to the a posteriori analysis of the time discretization. The efficiency and reliability of the spatial error estimator are established in Section 5. The a posteriori analysis of the full discrete problem is considered in Section 6, where we show the efficiency and reliability of the sum of

Math. classification: 65M15, 65M50, 65M60.
Keywords: Sobolev equations, a posteriori error analysis.

the spatial and time error estimators. Finally Section 7 is devoted to numerical tests which confirm our theoretical analysis.

Let us finish this section with some notations used in the remainder of the paper. For a bounded domain D, the usual norm and semi-norm of $H^s(D)$ ($s \geqslant 0$) are denoted by $\|\cdot\|_{s,D}$ and $|\cdot|_{s,D}$, respectively. For $s = 0$, we will drop the index s. Furthermore, the inner product in $L^2(\Omega)$ will be denoted by $(\cdot,\cdot)$. Finally, the notation $A \lesssim B$ (resp. $A \gtrsim B$) means the existence of a positive constant C_1 (resp. C_2), which is independent of A and B as well as the discretization parameters h and τ_p such that $A \leqslant C_1 B$ (resp. $A \geqslant C_2 B$). The notation $A \sim B$ means that $A \lesssim B$ and $A \gtrsim B$ hold simultaneously.

2. The continuous, time semi-discrete and full discrete problems

Let Ω be an open bounded of $\mathbb{R}^d$, $d = 2$ or 3, with a polygonal ($d = 2$) or polyhedral ($d = 3$) boundary Γ. Let T be a positive and fixed real number.

For $i = 1, 2$, let L_i be a second order elliptic operator in the form

$$L_i(x, D_x)u = -\sum_{k,\ell=1}^{d} \partial_k(a_{k,\ell}^{(i)}(x)\partial_\ell u) + \sum_{k=1}^{d} b_k^{(i)}(x)\partial_k u + c^{(i)}(x)u,$$

where $a_{k,\ell}^{(i)} = a_{\ell,k}^{(i)}, b_k^{(i)}, c^{(i)} \in L^\infty(\Omega)$ and introduce the bilinear forms on $H_0^1(\Omega)$

$$a_i(u,v) = \int_\Omega \left(\sum_{k,\ell=1}^{d} a_{k,\ell}^{(i)}(x)\partial_\ell u\, \partial_k v + \sum_{k=1}^{d} b_k^{(i)}(x)\partial_k u\, v + c^{(i)}(x)u\, v \right) dx.$$

We suppose that a_1 and a_2 are symmetric, that a_2 is non negative, i.e.,

$$a_2(u,u) \geqslant 0 \quad \text{for all } u \in H_0^1(\Omega), \tag{2.1}$$

and that a_1 is coercive in $H_0^1(\Omega)$, namely there exists $\alpha > 0$ such that

$$a_1(u,u) \geqslant \alpha \|u\|_{1,\Omega}^2 \quad \text{for all } u \in H_0^1(\Omega). \tag{2.2}$$

In this setting, we consider the following Sobolev equation: Let u be the solution of

$$\begin{cases} L_1 u_t + L_2 u = f & \text{in } \Omega \times (0,T), \\ u(\cdot,t) = 0 & \text{on } \Gamma \times (0,T), \\ u(\cdot,0) = u_0 & \text{in } \Omega, \end{cases} \tag{2.3}$$

where u_t means the time derivative of u. The datum f is supposed to satisfy $f \in L^2(0,T;H^{-1}(\Omega))$ and the initial value $u_0 \in H_0^1(\Omega)$. Under these assumptions, problem (2.3) or equivalently

$$a_1(u_t(t),v) + a_2(u(t),v) = (f(t),v) \quad \text{for all } v \in H_0^1(\Omega) \text{ and a.e. } t \in (0,T) \tag{2.4}$$

has a unique (weak) solution in $C([0,T];H_0^1(\Omega))$, see [3]. This system is a linear Sobolev equation in Ω, where some a priori error analyses were performed in [1, 13, 17, 19, 20, 23] in some particular situations or with a kind of Neumann boundary conditions. Some a posteriori error analyses can be found in [17, 26].

Without loss of generality, we can assume that a_2 is also coercive in $H_0^1(\Omega)$, indeed by the change of unknown

$$\tilde{u}(\cdot,t) = e^{-\lambda t}u(\cdot,t),$$

for a positive real number λ, we see that (2.4) is equivalent to

$$a_1(\tilde{u}_t(t),v) + \tilde{a}_2(\tilde{u}(t),v) = (e^{-\lambda t}f(t),v) \quad \text{for all } v \in H_0^1(\Omega) \text{ and a.e. } t \in (0,T), \tag{2.5}$$

where

$$\tilde{a}_2(u,v) = a_2(u,v) + \lambda a_1(u,v) \quad \text{for all } u,v \in H_0^1(\Omega)$$

is clearly coercive in $H_0^1(\Omega)$ due to (2.1)-(2.2). Hence from now on we also suppose that a_2 is coercive and denote by

$$\|u\|_{a_i} = \sqrt{a_i(u,u)}, \quad \text{for all } u \in H_0^1(\Omega),$$

two equivalent norms of $H_0^1(\Omega)$. We further denote by $\|u\|_{-1}$ the norm in $H^{-1}(\Omega)$ obtained by using the duality with the second norm of $H_0^1(\Omega)$, in other words,

$$\|g\|_{-1} = \sup_{v\in H_0^1(\Omega), v\neq 0} \frac{|\langle g; v\rangle|}{\|v\|_{a_2}}, \quad \text{for all } g \in H^{-1}(\Omega),$$

where $\langle\cdot;\cdot\rangle$ means the duality pairing between $H^{-1}(\Omega)$ and $H_0^1(\Omega)$.

2.1. **Time discretization using implicit Euler's scheme.** We now suppose that $f \in C([0,T];H^{-1}(\Omega))$. We further introduce a partition of $[0,T]$ into subintervals $[t_{p-1},t_p]$, $1 \leqslant p \leqslant N$ such that $0 = t_0 < t_1 < \cdots < t_N = T$. Denote by $\tau_p = t_p - t_{p-1}$ the length of $[t_{p-1},t_p]$ and by $\tau = \max_p \tau_p$ the global time mesh size.

The semi-discrete approximation of the continuous problem (2.3) by an implicit Euler scheme consists in finding a sequence $(u^p)_{0\leqslant p\leqslant N}$ solution of

$$\begin{cases} L_1\left(\dfrac{u^p - u^{p-1}}{\tau_p}\right) + L_2u^p = f^p & \text{in } \Omega, \quad 1 \leqslant p \leqslant N, \\ u^p = 0 & \text{on } \Gamma, \quad 1 \leqslant p \leqslant N, \\ u^0 = u_0 & \text{in } \Omega, \end{cases} \tag{2.6}$$

with $f^p = f(\cdot,t_p)$. This problem admits a unique weak solution $u^p \in H_0^1(\Omega)$, whose variational formulation is

$$a_1(\frac{u^p - u^{p-1}}{\tau_p}, v) + a_2(u^p,v) = \int_\Omega f^p v, \quad \text{for all } v \in H_0^1(\Omega), \tag{2.7}$$

or equivalently

$$a_1(u^p,v) + \tau_p a_2(u^p,v) = a_1(u^{p-1},v) + \tau_p \int_\Omega f^p v, \quad \text{for all } v \in H_0^1(\Omega). \tag{2.8}$$

The unique solvability of the variational formulation (2.8) is clearly a direct consequence of the Lax-Milgram lemma.

Remark 2.1. — An a priori error analysis of the explicit Euler scheme

$$a_1(\frac{u^p-u^{p-1}}{\tau_p},v)+a_2(u^{p-1},v)=\int_\Omega f^{p-1}v,\quad \text{for all } v\in H_0^1(\Omega), \tag{2.9}$$

was considered in [3] since it is more appropriate for Sobolev equations. The a posteriori error analysis that we perform below for system (2.8) is immediately applicable to (2.9) since it can be re-written as

$$a_{1,p}(\frac{u^p-u^{p-1}}{\tau_p},v)+a_2(u^p,v)=\int_\Omega f^{p-1}v,\quad \text{for all } v\in H_0^1(\Omega),$$

where

$$a_{1,p}(u,v)=a_1(u,v)-\tau_p a_2(u,v),$$

that is coercive uniformly in p, if τ_p is small enough.

2.2. **Full discretization.** Problem (2.8) is now discretized by a conforming finite element method. For that purpose, for any $p=0,1,\cdots,N$, let us fix a conforming mesh T_{ph} of Ω which is regular in Ciarlet's sense [9, p. 124]. All elements are triangles or tetrahedra and will be denoted by K. For an element $K\in T_{ph}$, we recall that h_K is the diameter of K and that $h_p=\max\limits_{K\in T_{ph}} h_K$. The set of all edges/faces of T_{ph} is denoted by $\mathcal{E}_{ph}$. Let $\mathcal{E}_{ph}^{\rm int}$ be the set of interior edges/faces of T_{ph} and $\mathcal{E}_K$ be the set of the edges/faces of the element K. Finally for an edge/face $E\in\mathcal{E}_K\cap\mathcal{E}_L$ we denote by $h_E=\frac{d}{2}(\frac{|K|}{|E|}+\frac{|L|}{|E|})$, its mean height.

Introduce the conforming finite element space:

$$V_{ph}=\{v\in H_0^1(\Omega): v_{|K}\in\mathbb{P}_1,\ \text{ for all } K\in T_{ph}\}.$$

The fully discrete approximation of problem (2.3) using Euler's scheme and the conforming finite element is then given by: Given an approximation $u_h^0\in V_{0h}$ of u_0, find $u_h^p\in V_{ph}$, $1\leqslant p\leqslant N$, such that

$$a_1(\frac{u_h^p-u_h^{p-1}}{\tau_p},v_h)+a_2(u_h^p,v_h)=\int_\Omega f^p v_h,\quad \text{for all } v_h\in V_{ph}, \tag{2.10}$$

or equivalently

$$a_1(u_h^p,v_h)+\tau_p a_2(u_h^p,v_h)=a_1(u_h^{p-1},v_h)+\tau_p\int_\Omega f^p v_h,\quad \text{for all } v_h\in V_{ph}. \tag{2.11}$$

Definition 2.2. — Let u^p be a solution of (2.8) and u_h^p a solution of (2.11), then we denote the spatial error by

$$e^p=u^p-u_h^p.$$

3. Some useful notations and properties

For a boundary edge/face E we denote the outward normal vector by n_E. Given an interior edge/face E, we choose an arbitrary normal direction n_E and denote by K_{in} and K_{ext} the two elements sharing this edge/face. Without any restriction, we may suppose here that n_E is pointing to K_{ext} like in Figure 3.1.

The jump of a function v across an edge/face E at a point x is defined by

$$[\![v(x)]\!]_E=\begin{cases}\lim\limits_{\alpha\to0^+}(v(x+\alpha n_E)-v(x-\alpha n_E)) & \text{if } E\in\mathcal{E}_{ph}^{\rm int},\\ v(x) & \text{if } E\in\mathcal{E}_{ph}\setminus\mathcal{E}_{ph}^{\rm int}.\end{cases}$$

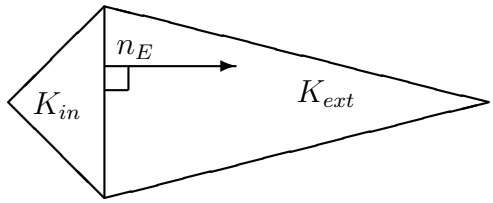

FIGURE 3.1. Two elements sharing the edge E

Note that the sign of $\big[\![v(x)]\!\big]_E$ depends on the orientation of n_E. However, quantity like a gradient jump $\big[\![\nabla v \cdot n_E]\!\big]_E$ is independent of this orientation.

In the sequel we will use local patches: for an element K we define ω_K as the union of all elements having a common edge/face with K, for an edge/face E, let ω_E be the union of both elements having E as an edge/face and finally for a node x, let ω_x be the union of all elements having x as a node. Similarly denote by $\tilde{\omega}_K$ (resp. $\tilde{\omega}_E$) the union of all triangles sharing a node with K (resp. E).

Recall that the Clément interpolation operator is defined as follows: Denote by $\mathcal{N}_{ph}$ the set of nodes of the triangulation T_{ph} and by $\mathcal{N}_{ph}^{\rm int}$ the set of interior nodes of the triangulation T_{ph}. For each node $x \in \mathcal{N}_{ph}^{\rm int}$ denote further by λ_x the standard hat function associated with x, namely $\lambda_x \in V_{ph}$ and satifies

$$\lambda_x(y) = \delta_{x,y}, \quad \text{for all } y \in \mathcal{N}_{ph}^{\rm int}.$$

For any $w \in L^2(\Omega)$, we define $I_C^0 w$ by

$$I_C^0 w = \sum_{x \in \mathcal{N}_{ph}^{\rm int}} |\omega_x|^{-1} \Big(\int_{\omega_x} w \Big) \lambda_x. \tag{3.1}$$

Note that $I_C^0 w$ belongs to V_{ph}. Moreover this operator has the following properties [10]:

LEMMA 3.1. — *For all $w \in H_0^1(\Omega)$, we have*

$$\|w - I_C^0 w\|_K \lesssim h_K \|\nabla w\|_{\tilde{\omega}_K}, \qquad \text{for all } K \in T_{ph}, \tag{3.2}$$

$$\|w - I_C^0 w\|_E \lesssim h_E^{1/2} \|\nabla w\|_{\tilde{\omega}_E}, \qquad \text{for all } E \in \mathcal{E}_{ph}^{\rm int}, \tag{3.3}$$

$$\|\nabla I_C^0 w\|_K \lesssim \|\nabla w\|_{\tilde{\omega}_K}, \qquad \text{for all } K \in T_{ph}. \tag{3.4}$$

If $K \in T_{ph}$, then the element residual is defined on K by

$$R_K^p = \Big(f(\cdot, t_p) - L_1\big(\frac{u_h^p - u_h^{p-1}}{\tau_p}\big) - L_2 u_h^p \Big)_{|K},$$

while if $E \in \mathcal{E}_{ph}^{\rm int}$, then the edge/face residual is

$$J_{E,n}^p = \Big[\!\!\Big[\Big(A_1 \nabla \Big(\tfrac{u_h^p - u_h^{p-1}}{\tau_p} \Big) + A_2 \nabla u_h^p \Big) \cdot n_E \Big]\!\!\Big]_E,$$

where for $i = 1$ or 2, A_i is the $d \times d$ symmetric matrix given by

$$A_i = (a_{k,\ell}^{(i)})_{1 \leqslant k,\ell \leqslant d}.$$

Now we prove a property satisfied by the spatial error e^p that we will use in the proof of the spatial error bounds.

LEMMA 3.2 (Galerkin orthogonality). — *The error e^p satisfies the Galerkin orthogonality relation*

$$a_1(\frac{e^p-e^{p-1}}{\tau_p},v_h)+a_2(e^p,v_h)=0,\qquad \text{for all } v_h\in V_{ph}. \tag{3.5}$$

Proof. — It suffices to subtract (2.7) with $v=v_h\in V_{ph}$ to the identity (2.10). □

LEMMA 3.3. — *The error e^p satisfies*

$$a_1(\frac{e^p-e^{p-1}}{\tau_p},v)+a_2(e^p,v)=\sum_{K\in T_{ph}}\int_K R_K^p v+\sum_{E\in\mathcal{E}_{ph}^{\rm int}}\int_E J_{E,n}^p v,\qquad \text{for all } v\in H_0^1(\Omega). \tag{3.6}$$

Proof. — We first observe that

$$a_1(\frac{e^p-e^{p-1}}{\tau_p},v)+a_2(e^p,v)=a_1(\frac{u^p-u^{p-1}}{\tau_p},v)+a_2(u^p,v)\\ -\left(a_1(\frac{u_h^p-u_h^{p-1}}{\tau_p},v)+a_2(u_h^p,v)\right).$$

We transform the first term on the right-hand side using (2.7) and the second one by elementwise integration by parts, reminding that

$$a_i(u,v)=\sum_{K\in T_{ph}}\int_K\left((A_i\nabla u\cdot\nabla v+\sum_{k=1}^d b_k^{(i)}\partial_k uv+c^{(i)}uv\right).$$

This leads to the conclusion. □

The above lemmas allow us to prove the following lemma.

LEMMA 3.4. — *The following identity holds*

$$a_1(e^p,e^p)+\tau_p a_2(e^p,e^p)=a_1(e^{p-1},e^p)+\tau_p\sum_{K\in T_{ph}}\int_K R_K^p(e^p-I_C^0e^p)\\ +\tau_p\sum_{E\in\mathcal{E}_{ph}^{\rm int}}\int_E J_{E,n}^p(e^p-I_C^0e^p). \tag{3.7}$$

Proof. — We write

$$a_2(e^p,e^p)=a_2(e^p,e^p-I_C^0e^p)+a_2(e^p,I_C^0e^p),$$

then we transform the first term using (3.6) with $v=e^p-I_C^0e^p$ and the second term using the Galerkin orthogonality relation (3.5) with $v_h=I_C^0e^p$. □

4. A posteriori analysis of the time discretization

Inspired from [4, 6, 16, 18, 21], that considered the heat equation, we define the time error indicator by

$$\eta_t^p=\tau_p^{1/2}\|u_h^p-u_h^{p-1}\|_{a_2},1\leqslant p\leqslant N. \tag{4.1}$$

The only difference with the above papers lies on the chosen norm of $u_h^p-u_h^{p-1}$.

For shortness we introduce the following notation: Denote by $\pi_\tau f$ the step function which is constant and equal to $f(t_p)$ on each interval (t_{p-1},t_p), $1\leqslant p\leqslant N$. For

a sequence $v^p \in H_0^1(\Omega)$, $0 \leqslant p \leqslant N$, we denote by v_τ its "Lagrange" interpolant, which is affine on each interval $[t_{p-1}, t_p]$, $1 \leqslant p \leqslant N$, and equal to v^p at t_p, i.e., defined by,

$$v_\tau(t) = \frac{t_p - t}{\tau_p} v^{p-1} + \frac{t - t_{p-1}}{\tau_p} v^p, \quad \text{for all } t \in [t_{p-1}, t_p], 1 \leqslant p \leqslant N.$$

Denote finally $e_\tau = u - u_\tau$, the time discretization error.

As

$$\partial_t u_\tau = \frac{u^p - u^{p-1}}{\tau_p} \text{ on } (t_{p-1}, t_p),$$

the semi-discrete equation (2.7) is equivalent to

$$a_1(\partial_t u_\tau(t), v) + a_2(u^p, v) = (f^p, v), \quad \text{for all } v \in H_0^1(\Omega) \text{ and all } t \in (t_{p-1}, t_p). \tag{4.2}$$

Taking the difference with (2.4), we derive the residual equation

$$a_1(\partial_t e_\tau(t), v) + a_2(e_\tau(t), v) = ((f - \pi_\tau f)(t), v) + a_2((u^p - u_\tau)(t), v), \tag{4.3}$$

for all $v \in H_0^1(\Omega)$ and a.e. $t \in (t_{p-1}, t_p)$.

This identity allows us to prove the next error bound.

THEOREM 4.1 (Time upper error bound). — *The next estimate holds*

$$\|e_\tau(t_n)\|_{a_1}^2 + \int_0^{t_n} \|e_\tau(s)\|_{a_2}^2 \, ds \lesssim \tag{4.4}$$
$$\sum_{p=1}^{n} (\eta_t^p)^2 + \int_0^{t_n} \|(u_\tau - u_{h\tau})(s)\|_{a_2}^2 \, ds + \|f - \pi_\tau f\|^2_{L^2(0,t_n;H^{-1}(\Omega))}.$$

Proof. — The residual equation (4.3) with $v = e_\tau(t)$ yields

$$a_1(\partial_t e_\tau(t), e_\tau(t)) + a_2(e_\tau(t), e_\tau(t)) = ((f - \pi_\tau f)(t), e_\tau(t)) + a_2((u^p - u_\tau)(t), e_\tau(t)),$$

for a.e. $t \in (t_{p-1}, t_p)$. As a_1 is symmetric, we have

$$a_1(\partial_t e_\tau(t), e_\tau(t)) = \frac{1}{2} \partial_t a_1(e_\tau(t), e_\tau(t)),$$

hence integrating the above identity in $t \in (t_{p-1}, t_p)$, one gets

$$\frac{1}{2} a_1(e_\tau(t_p), e_\tau(t_p)) - \frac{1}{2} a_1(e_\tau(t_{p-1}), e_\tau(t_{p-1})) + \int_{t_{p-1}}^{t_p} a_2(e_\tau(t), e_\tau(t))$$
$$= \int_{t_{p-1}}^{t_p} ((f - \pi_\tau f)(t), e_\tau(t)) \, dt + \int_{t_{p-1}}^{t_p} a_2((u^p - u_\tau)(t), e_\tau(t)) \, dt.$$

Using Young's inequality, one obtains

$$\frac{1}{2} a_1(e_\tau(t_p), e_\tau(t_p)) - \frac{1}{2} a_1(e_\tau(t_{p-1}), e_\tau(t_{p-1})) + \frac{1}{2} \int_{t_{p-1}}^{t_p} a_2(e_\tau(t), e_\tau(t)) \tag{4.5}$$
$$\leqslant \int_{t_{p-1}}^{t_p} \|(f - \pi_\tau f)(t)\|_{-1}^2 \, dt + \int_{t_{p-1}}^{t_p} \|(u^p - u_\tau)(t)\|_{a_2}^2 \, dt.$$

We now estimate the second term of this right-hand side. First by the definition of u_τ we clearly have

$$\int_{t_{p-1}}^{t_p} \|(u^p - u_\tau)(t)\|_{a_2}^2 \, dt = \frac{\tau_p}{3} \|u^p - u^{p-1}\|_{a_2}^2. \tag{4.6}$$

Secondly, using the triangular inequality, we simply write

$$\tau_p^{1/2}\|u^p-u^{p-1}\|_{a_2}\leqslant \eta_t^p+\tau_p^{1/2}\|u^p-u_h^p\|_{a_2}+\tau_p^{1/2}\|u_h^{p-1}-u^{p-1}\|_{a_2}. \tag{4.7}$$

Let us now show that

$$\tau_p\|u^p-u_h^p\|_{a_2}^2+\tau_p\|u^{p-1}-u_h^{p-1}\|_{a_2}^2\leqslant 6\int_{t_{p-1}}^{t_p}\|(u_\tau-u_{h\tau})(t)\|_{a_2}^2\,dt. \tag{4.8}$$

Indeed by definition, we have

$$(u_\tau-u_{h\tau})(t)=\frac{t_p-t}{\tau_p}(u^{p-1}-u_h^{p-1})+\frac{t-t_{p-1}}{\tau_p}(u^p-u_h^p),\quad \text{for all } t\in[t_{p-1},t_p],$$

and therefore

$$\begin{aligned}\|(u_\tau-u_{h\tau})(t)\|_{a_2}^2=&\left(\frac{t_p-t}{\tau_p}\right)^2\|u^{p-1}-u_h^{p-1}\|_{a_2}^2+\left(\frac{t-t_{p-1}}{\tau_p}\right)^2\|u^p-u_h^p\|_{a_2}^2\\&+2\frac{(t_p-t)(t-t_{p-1})}{\tau_p^2}a_2(u^{p-1}-u_h^{p-1},u^p-u_h^p),\end{aligned}$$

for all $t\in(t_{p-1},t_p)$.

Integrating this expression in $t\in(t_{p-1},t_p)$, one finds after simple calculations that

$$\begin{aligned}&\int_{t_{p-1}}^{t_p}\|(u_\tau-u_{h\tau})(t)\|_{a_2}^2\,dt=\\&\qquad\frac{\tau_p}{3}(\|u^{p-1}-u_h^{p-1}\|_{a_2}^2+\|u^p-u_h^p\|_{a_2}^2+a_2(u^{p-1}-u_h^{p-1},u^p-u_h^p)).\end{aligned}$$

Cauchy-Schwarz's inequality allows to conclude that (4.8) holds.

In conclusion, the identity (4.6) and the estimates (4.7)-(4.8) yield

$$\int_{t_{p-1}}^{t_p}\|(u^p-u_\tau)(t)\|_{a_2}^2\,dt\lesssim(\eta_t^p)^2+\int_{t_{p-1}}^{t_p}\|(u_\tau-u_{h\tau})(t)\|_{a_2}^2\,dt. \tag{4.9}$$

This estimate in (4.5) leads to

$$\begin{aligned}&a_1(e_\tau(t_p),e_\tau(t_p))-a_1(e_\tau(t_{p-1}),e_\tau(t_{p-1}))+\int_{t_{p-1}}^{t_p}a_2(e_\tau(t),e_\tau(t))\\&\qquad\lesssim(\eta_t^p)^2+\int_{t_{p-1}}^{t_p}\|(f-\pi_\tau f)(t)\|_{-1}^2\,dt+\int_{t_{p-1}}^{t_p}\|(u_\tau-u_{h\tau})(t)\|_{a_2}^2\,dt.\end{aligned}$$

Summing this estimate in $p=1,\cdots,n$ leads to the conclusion. □

Corollary 4.2 (Second time upper error bound). — *The next estimate holds*

$$\|\partial_t e_\tau\|_{L^2(0,t_n;H_0^1(\Omega))}^2\lesssim\sum_{p=1}^n(\eta_t^p)^2+\int_0^{t_n}\|(u_\tau-u_{h\tau})(s)\|_{a_2}^2\,ds+\|f-\pi_\tau f\|_{L^2(0,t_n;H^{-1}(\Omega))}^2. \tag{4.10}$$

Proof. — The residual equation (4.3) and the equivalence between the norms $\|\cdot\|_{a_1}$ and $\|\cdot\|_{a_2}$ directly give

$$\|\partial_t e_\tau(t)\|_{a_1}\lesssim\|(f-\pi_\tau f)(t)\|_{-1}+\|e_\tau(t)\|_{a_2}+\|(u^p-u_\tau)(t)\|_{a_2},$$

for all $t\in(t_{p-1},t_p)$.

Integrating the square of this estimate in $t \in (t_{p-1}, t_p)$ and summing on p, we obtain

$$\int_0^{t_n} \|\partial_t e_\tau(t)\|_{a_1}^2 \, dt \lesssim \int_0^{t_n} \|(f - \pi_\tau f)(t)\|_{-1}^2 \, dt + \int_0^{t_n} \|e_\tau(t)\|_{a_2}^2 \, dt + \int_0^{t_n} \|(u^p - u_\tau)(t)\|^2 \, dt.$$

The second term of this right-hand side is estimated in (4.4), while the third term is estimated via (4.9). □

Remark 4.3. — In the implementation point of view, all the terms of the right-hand side of (4.4) and of (4.10) should be computable. This is indeed the case for the terms $(\eta_t^p)^2$ and $\|f - \pi_\tau f\|^2_{L^2(0,t_n;H^{-1}(\Omega))}$, while the term $\int_0^{t_n} \|(u_\tau - u_{h\tau})(s)\|_{a_2}^2 \, ds$ is not, because the exact solutions u^p are used, but it will be estimated by computational quantities in the next section (see Theorem 5.2 and the estimate (6.3) below).

Let us go on with the local time lower bound.

THEOREM 4.4 (Time lower error bound). — *For all $p = 1, \cdots, N$, the next estimate holds*

$$(\eta_t^p)^2 \lesssim \int_{t_{p-1}}^{t_p} (\|e_\tau(t)\|_{a_2}^2 + \|\partial_t e_\tau(t)\|_{a_1}^2) \, dt + \tau_p(\|u^p - u_h^p\|_{a_2}^2 + \|u^{p-1} - u_h^{p-1}\|_{a_2}^2) + \|f - \pi_\tau f\|^2_{L^2(t_{p-1},t_p;H^{-1}(\Omega))}. \tag{4.11}$$

Proof. — By the triangular inequality we may write

$$\eta_t^p \lesssim \tau_p^{1/2}(\|u^p - u^{p-1}\|_{a_2} + \|u^p - u_h^p\|_{a_2} + \|u^{p-1} - u_h^{p-1})\|_{a_2}). \tag{4.12}$$

Hence it remains to estimate the term $\tau_p^{1/2}\|u^p - u^{p-1}\|_{a_2}$. First we recall the identity (4.6)

$$\frac{\tau_p}{3}\|u^p - u^{p-1}\|_{a_2}^2 = \int_{t_{p-1}}^{t_p} \|(u^p - u_\tau)(t)\|_{a_2}^2 \, dt.$$

Second taking as test function in (4.3) $v = (u^p - u_\tau)(t)$, with $t \in (t_{p-1}, t_p)$, one obtains

$$a_1(\partial_t e_\tau(t), (u^p - u_\tau)(t)) + a_2(e_\tau(t), (u^p - u_\tau)(t)) = ((f - \pi_\tau f)(t), (u^p - u_\tau)(t)) + a_2((u^p - u_\tau)(t), (u^p - u_\tau)(t)),$$

for a.e. $t \in (t_{p-1}, t_p)$.

With the help of Cauchy-Schwarz's inequality and the continuity of a_1 and the coerciveness of a_2, we arrive at

$$\|(u^p - u_\tau)(t)\|_{a_2}^2 \lesssim \|\partial_t e_\tau(t)\|_{a_1}^2 + \|e_\tau(t)\|_{a_2}^2 + \|(f - \pi_\tau f)(t)\|_{-1}^2,$$

for all a.e. $t \in (t_{p-1}, t_p)$. Integrating this estimate in $t \in (t_{p-1}, t_p)$ we deduce that

$$\frac{\tau_p}{3}\|u^p - u^{p-1}\|_{a_2}^2 \lesssim \int_{t_{p-1}}^{t_p} (\|e_\tau(t)\|_{a_2}^2 + \|\partial_t e_\tau(t)\|_{a_1}^2 + \|f - \pi_\tau f\|_{-1}^2) \, dt.$$

The conclusion follows by inserting this estimate in (4.12). □

5. A posteriori analysis of the spatial discretization

5.1. **An upper error bound.** As usual [27] the exact element residual R_K^p it is replaced by an approximate element residual

$$r_K^p = \Big((f_h^p - L_1\big(\frac{u_h^p - u_h^{p-1}}{\tau_p}\big) - L_2 u_h^p\Big)_{|K}, \tag{5.1}$$

where f_h^p is a finite dimensional approximation of $f(\cdot, t_p)$. A possible choice is $(f_h^p)_{|K} := \dfrac{1}{|K|}\displaystyle\int_K f(x,t_p)\,dx$, for all $K \in T_{ph}$.

Definition 5.1. — Let $p \geqslant 1$. The local error estimator η_K^p is defined by

$$\eta_K^p = h_K \|r_K^p\|_K + \sum_{E\in\mathcal{E}_K} h_E^{1/2} \left\|J_{E,n}^p\right\|_E,$$

while the global one η^p is given by

$$(\eta^p)^2 = \sum_{K\in T_{ph}} (\eta_K^p)^2.$$

The local and global approximation terms are defined by

$$\xi_K^p = h_K \|f(\cdot,t_p) - f_h^p\|_{\omega_K}, \quad (\xi^p)^2 = \sum_{K\in T_{ph}} (\xi_K^p)^2.$$

Theorem 5.2 (Upper error bound). — *The next estimate holds*

$$\|e^n\|_{a_1}^2 + \sum_{p=1}^n \tau_p \|e^p\|_{a_2}^2 \lesssim \sum_{p=1}^n \tau_p((\eta^p)^2 + (\xi^p)^2) + \|e^0\|_{a_1}^2. \tag{5.2}$$

Proof. — This upper bound is a consequence of Lemma 3.4 by estimating appropriately each term of the right-hand side of the identity (3.7). First we transform

$$\begin{aligned}\tau_p \sum_{K\in T_{ph}} \int_K R_K^p (e^p - I_C^0 e^p) = \tau_p \sum_{K\in T_{ph}} \int_K r_K^p (e^p - I_C^0 e^p) \\ + \tau_p \sum_{K\in T_{ph}} \int_K (f(\cdot,t_p) - f_h^p)(e^p - I_C^0 e^p).\end{aligned}$$

Using successively Cauchy-Schwarz's inequality, the estimate (3.2) and the definition 5.1 of the local estimator and the approximation term, we obtain

$$\begin{aligned}\sum_{K\in T_{ph}} \int_K R_K^p (e^p - I_C^0 e^p) &\lesssim \sum_{K\in T_{ph}} h_K (\|r_K^p\|_K + \|f(\cdot,t_p) - f_h^p\|_K)\, |e^p|_{1,\tilde{\omega}_K} \\ &\lesssim \sum_{K\in T_{ph}} (\eta_K^p + \xi_K^p)\, |e^p|_{1,\tilde{\omega}_K}.\end{aligned}$$

By discrete Cauchy-Schwarz's inequality and the coerciveness of a_2, we get

$$\sum_{K\in T_{ph}} \int_K R_K^p (e^p - I_C^0 e^p) \lesssim (\eta^p + \xi^p)\, |e^p|_{1,\Omega} \lesssim (\eta^p + \xi^p) \|e^p\|_{a_2}. \tag{5.3}$$

Similarly using (3.3) we estimate the edge residual term:

$$\begin{aligned}\sum_{E\in\mathcal{E}_{ph}^{\mathrm{int}}}\int_E J_{E,n}^p(e^p - I_C^0 e^p) &\leqslant \sum_{E\in\mathcal{E}_{ph}^{\mathrm{int}}}\left\|J_{E,n}^p\right\|_E \left\|e^p - I_C^0 e^p\right\|_E\\ &\lesssim \sum_{E\in\mathcal{E}_{ph}^{\mathrm{int}}}\left\|J_{E,n}^p\right\|_E h_E^{1/2}\,|e^p|_{1,\tilde{\omega}_E}\\ &\lesssim \sum_{K\in T_{ph}} \eta_K^p\,|e^p|_{1,\tilde{\omega}_K}\,.\end{aligned}$$

As before discrete Cauchy-Schwarz's inequality yields

$$\sum_{E\in\mathcal{E}_{ph}^{\mathrm{int}}}\int_E J_{E,n}^p(e^p - I_C^0 e^p) \lesssim \eta^p\,|e^p|_{1,\Omega} \lesssim \eta^p \|e^p\|_{a_2}. \tag{5.4}$$

Applying Cauchy-Schwarz's and Young's inequalities we get

$$a_1(e^{p-1}, e^p) \leqslant \frac{1}{2}(\|e^{p-1}\|_{a_1}^2 + \|e^p\|_{a_1}^2).$$

This estimate and (5.3), (5.4) in the identity (3.7) yield

$$\begin{aligned}\|e^p\|_{a_1}^2 + \tau_p\|e^p\|_{a_2}^2 &\leqslant \frac{1}{2}(\|e^{p-1}\|_{a_1}^2 + \|e^p\|_{a_1}^2) + C\tau_p(\eta^p + \xi^p)\|e^p\|_{a_2}\\ &\leqslant \frac{1}{2}(\|e^{p-1}\|_{a_1}^2 + \|e^p\|_{a_1}^2) + \frac{C^2}{2}\tau_p(\eta^p + \xi^p)^2 + \frac{1}{2}\tau_p\|e^p\|_{a_2}^2,\end{aligned}$$

for some constant $C > 0$ depending only on the minimal angle of T_{ph}, where in the second step we again use Young's inequality. After simplification, this estimate is equivalent to

$$\|e^p\|_{a_1}^2 + \tau_p\|e^p\|_{a_2}^2 \leqslant \|e^{p-1}\|_{a_1}^2 + C^2\tau_p(\eta^p + \xi^p)^2,$$

and we conclude by taking the sum on $p = 1, \ldots, n$. □

Corollary 5.3 (Second upper error bound). — *The next estimate holds*

$$\|\partial_t(u_\tau - u_{h\tau})\|_{L^2(0,t_n;H_0^1(\Omega)}^2 \lesssim \sum_{p=1}^n \tau_p((\eta^p)^2 + (\xi^p)^2) + \|e^0\|_{a_1}^2. \tag{5.5}$$

Proof. — By the coerciveness of a_1, we have

$$\|\partial_t(u_\tau - u_{h\tau})(t)\|_{a_1} \leqslant \sup_{v\in H_0^1(\Omega)} \frac{a_1(\partial_t(u_\tau - u_{h\tau})(t), v)}{\|v\|_{a_1}}, \quad \text{for all } t \in (t_{p-1}, t_p). \tag{5.6}$$

Using the property

$$\partial_t(u_\tau - u_{h\tau})(t) = \frac{e^p - e^{p-1}}{\tau_p}, \quad \text{for all } t \in (t_{p-1}, t_p),$$

and the semi-discrete equation (2.8), for any $t \in (t_{p-1}, t_p)$ we may write

$$a_1(\partial_t(u_\tau - u_{h\tau})(t), v) = R^p(v) - a_2(e^p, v),$$

where the residual R^p is defined by

$$R^p(v) = (f(\cdot, t_p), v) - a_1(\frac{u_h^p - u_h^{p-1}}{\tau_p}, v) - a_2(u_h^p, v), \quad \text{for all } v \in H_0^1(\Omega).$$

As (2.11) implies that

$$R^p(v_h) = 0, \quad \text{for all } v_h \in V_{ph},$$

the above identity becomes

$$a_1(\partial_t(u_\tau - u_{h\tau})(t), v) = R^p(v - v_h) - a_2(e^p, v), \quad \text{for all } v_h \in V_{ph}, t \in (t_{p-1}, t_p).$$

Taking $v_h = I_C v$, applying Green's formula componentwise (see the proof of Lemma 3.3), and using the estimates (3.2) and (3.3) we get

$$|R^p(v - v_h)| \lesssim (\eta^p + \xi^p)\|v\|_{a_1},$$

and therefore

$$|a_1(\partial_t(u_\tau - u_{h\tau})(t), v)| \lesssim (\eta^p + \xi^p + \|e^p\|_{a_2})\|v\|_{a_1}, \quad \text{for all } t \in (t_{p-1}, t_p).$$

This estimate in (5.6) leads to

$$\|\partial_t(u_\tau - u_{h\tau})(t)\|_{a_1} \lesssim \eta^p + \xi^p + \|e^p\|_{a_2}.$$

Integrating the square of this estimate in $t \in (t_{p-1}, t_p)$ and summing on $p = 1, \cdots, n$, the conclusion follows from the estimate (5.2). □

5.2. **A lower error bound.** We now establish the lower error bound of the estimator η_K^p in a more or less standard way (see [27]). Since we consider a nonstationary problem, we further need the following assumption (see [6, 29]), that is easily checked in an adaptive context:

Assumption 5.4. — *For each $1 \leqslant p \leqslant N$, there exists a conforming triangulation $\tilde{T}_{ph}$ such that each element K of $T_{p-1,h}$ or of T_{ph} is the union of elements $\tilde{K}$ of $\tilde{T}_{ph}$ such that $h_K \sim h_{\tilde{K}}$.*

We further need the assumption on the coefficients of the operators L_i.

Assumption 5.5. — *For each $1 \leqslant p \leqslant N$, and $i = 1, 2$, the coefficients $a_{k,\ell}^{(i)}, b_k^{(i)}$ and $c^{(i)}$ are constant on each element K of $\tilde{T}_{ph}$.*

Theorem 5.6 (Local lower error bound). — *If Assumptions 5.4 and 5.5 hold, then for all $1 \leqslant p \leqslant N$ and all $K \in T_{ph}$, one has*

$$\eta_K^p \lesssim h_K \|\frac{e^p - e^{p-1}}{\tau_p}\|_{1,\omega_K} + \|e^p\|_{1,\omega_K} + \sum_{K' \subset \omega_K} \xi_{K'}^p. \tag{5.7}$$

Proof. — **Element residual:** By fixing an arbitrary element $K \in \tilde{T}_{ph}$ and by recalling (5.1), we set

$$w_K^p := b_K r_K^p,$$

where $b_K = \prod_{i=1}^{d+1} \lambda_i^K$ is the standard bubble function associated with K (see e.g. [27]). Standard inverse inequalities (cf. [27, Lemma 3.3]) and Lemma 3.3 with $v = w_K^p$ give

$$\begin{aligned}\|r_K^p\|_K^2 \sim \int_K r_K^p w_K^p &= \int_K (f_h^p - f(\cdot, t_p)) w_K^p + \int_K R_K^p w_K^p \\ &= \int_K (f_h^p - f(\cdot, t_p)) w_K^p + a_1(\frac{e^p - e^{p-1}}{\tau_p}, w_K^p) + a_2(e^p, w_K^p).\end{aligned}$$

Hence by Cauchy-Schwarz's inequality and again standard inverse inequalities (reminding that u_h^{p-1} and u_h^p are polynomials of degree 1 in K, see again [27, Lemma 3.3]), one obtains

$$\|r_K^p\|_K^2 \lesssim (\|\frac{e^p - e^{p-1}}{\tau_p}\|_{1,K} + h_K^{-1}\|e^p\|_{1,K} + \|f_h^p - f(\cdot,t_p)\|_K)\|r_K^p\|_K.$$

This proves the estimate

$$h_K\|r_K^p\|_K \lesssim h_K\|\frac{e^p - e^{p-1}}{\tau_p}\|_{1,K} + \|e^p\|_{1,K} + h_K\|f_h^p - f(\cdot,t_p)\|_K. \tag{5.8}$$

Now for $K \in T_{ph}$, the assumption 5.4 yields

$$h_K^2\|r_K^p\|_K^2 \lesssim \sum_{\tilde{K}\in\tilde{T}_{ph}:\tilde{K}\subset K} h_{\tilde{K}}^2\|r_{\tilde{K}}^p\|_{\tilde{K}}^2.$$

Using the estimate (5.8) and the fact that $h_{\tilde{K}} \leqslant h_K$ for $\tilde{K} \subset K$ we have proved that

$$h_K\|r_K^p\|_K \lesssim h_K\|\frac{e^p - e^{p-1}}{\tau_p}\|_{1,K} + \|e^p\|_{1,K} + \xi_K^p. \tag{5.9}$$

Edge/face residual: Next we consider an arbitrary edge/face E of $\tilde{T}_{ph}$ and define

$$w_E^p := b_E J_{E,n}^p,$$

where b_E is the standard bubble function associated with E (see e.g. [27]). Using inverse estimates and Lemma 3.3 with $v = w_E^p$ we obtain

$$\|J_{E,n}^p\|_E^2 \lesssim \int_E J_{E,n}^p w_E^p = a_1(\frac{e^p - e^{p-1}}{\tau_p}, w_E^p) + a_2(e^p, w_E^p) - \sum_{K\in\tilde{T}_{ph}}\int_K R_K^p w_E^p.$$

Hence Cauchy-Schwarz's inequality, standard inverse inequalities and the estimate (5.8) lead to

$$h_E^{1/2}\left\|J_{E,n}^p\right\|_E \lesssim \sum_{K\in\tilde{T}_{ph}:E\subset K} (\|\frac{e^p - e^{p-1}}{\tau_p}\|_{1,K} + \|e^p\|_{1,K} + h_K\|f_h^p - f(\cdot,t_p)\|_K).$$

By the assumption 5.4, we conclude that

$$h_E^{1/2}\left\|J_{E,n}^p\right\|_E \lesssim \sum_{K\subset\omega_E} (\|\frac{e^p - e^{p-1}}{\tau_p}\|_{1,K} + \|e^p\|_{1,K} + \xi_K^p). \tag{5.10}$$

The conclusion follows from the estimates (5.9) and (5.10). □

Corollary 5.7 (Second local lower error bound). — *If Assumptions 5.4 and 5.5 hold, then for all $1 \leqslant p \leqslant N$ and all $K \in T_{ph}$, it holds*

$$\tau_p(\eta_K^p)^2 \lesssim \int_{t_{p-1}}^{t_p} \|\partial_t(u_\tau - u_{h\tau})(t)\|_{1,\omega_K}^2\, dt + \tau_p\|e^p\|_{1,\omega_K}^2 + \tau_p \sum_{K'\subset\omega_K} (\xi_{K'}^p)^2. \tag{5.11}$$

Proof. — Direct consequence of the property

$$\partial_t(u_\tau - u_{h\tau})(t) = \frac{e^p - e^{p-1}}{\tau_p}, \quad \text{for all } t \in (t_{p-1}, t_p),$$

and Theorem 5.6. □

6. A posteriori analysis of the full discretization

For all $n = 1, \cdots, N$, denote the full error $E(t_n)$ at time t_n by

$$\begin{aligned} E(t_n)^2 &= \|u(t_n) - u_h^n\|_{a_1}^2 + \|u^n - u_h^n\|_{a_1}^2 \\ &\quad + \|\partial_t(u - u_\tau)\|_{L^2(0,t_n;H_0^1(\Omega))}^2 + \|\partial_t(u_\tau - u_{h\tau})\|_{L^2(0,t_n;H_0^1(\Omega))}^2 \\ &\quad + \int_0^{t_n} (\|(u - u_\tau)(\cdot,s)\|_{a_2}^2 + \|(u_\tau - u_{h\tau})(\cdot,s)\|_{a_2}^2)\, ds. \end{aligned}$$

Combining the results from the previous sections, we get the following global upper and lower bounds:

Theorem 6.1 (Full error bounds). — *For any $n = 1, \cdots, N$, the next upper error bound holds:*

$$\begin{aligned} E(t_n)^2 &\lesssim \sum_{p=1}^{n} \left((\eta_t^p)^2 + \tau_p(\eta^p)^2\right) \\ &\quad + \|f - \pi_\tau f\|_{L^2(0,t_n;H^{-1}(\Omega))}^2 + \sum_{p=1}^{n} \tau_p(\xi^p)^2 + \|e^0\|_{a_1}^2 + \tau_1\|e^0\|_{a_2}^2. \end{aligned} \tag{6.1}$$

If moreover Assumptions 5.4 and 5.5 hold, then for any $n = 1, \cdots, N$, the next lower error bound holds:

$$\sum_{p=1}^{n} \left((\eta_t^p)^2 + \tau_p(\eta^p)^2\right) \lesssim E(t_n)^2 + \|f - \pi_\tau f\|_{L^2(0,t_n;H^{-1}(\Omega))}^2 + \sum_{p=1}^{n} \tau_p(\xi^p)^2. \tag{6.2}$$

Proof. — Let us start with the upper error bound. First the triangle inequality directly leads to

$$\begin{aligned} E(t_n)^2 &\lesssim \|u(t_n) - u^n\|_{a_1}^2 + \|u^n - u_h^n\|_{a_1}^2 \\ &\quad + \|\partial_t e_\tau\|_{L^2(0,t_n;H_0^1(\Omega))}^2 + \|\partial_t(u_\tau - u_{h\tau})\|_{L^2(0,t_n;H_0^1(\Omega))}^2 \\ &\quad + \int_0^{t_n} (\|e_\tau(\cdot,s)\|_{a_2}^2 + \|(u_\tau - u_{h\tau})(\cdot,s)\|_{a_2}^2)\, ds. \end{aligned}$$

By Theorem 4.1 and Corollary 4.2, and the easily checked estimate

$$\int_0^{t_n} \|(u_\tau - u_{h\tau})(\cdot,s)\|_{a_2}^2\, ds \lesssim \sum_{p=1}^{n} \tau_p(\|u^{p-1} - u_h^{p-1}\|_{a_2}^2 + \|u^p - u_h^p\|_{a_2}^2), \tag{6.3}$$

we get

$$\begin{aligned} E(t_n)^2 &\lesssim \sum_{p=1}^{n} (\eta_t^p)^2 + \sum_{p=1}^{n} \tau_p\|u^p - u_h^p\|_{a_2}^2 \\ &\quad + \|f - \pi_\tau f\|_{L^2(0,t_n;H^{-1}(\Omega))}^2 + \|u^n - u_h^n\|_{a_1}^2 \\ &\quad + \|\partial_t(u_\tau - u_{h\tau})\|_{L^2(0,t_n;H_0^1(\Omega))}^2 + \tau_1\|e^0\|_{a_2}^2. \end{aligned}$$

We conclude using Theorem 5.2 and Corollary 5.3.

We now pass to the lower error bound. Summing (4.11) on $p = 1, \cdots, n$, we get

$$\begin{aligned} \sum_{p=1}^{n} (\eta_t^p)^2 &\lesssim \int_0^{t_n} (\|e_\tau(t)\|_{a_2}^2 + \|\partial_t e_\tau(t)\|_{a_1}^2)\, dt + \sum_{p=1}^{n} \tau_p\|u^p - u_h^p\|_{a_2}^2 + \tau_1\|e^0\|_{a_2}^2 \\ &\quad + \|f - \pi_\tau f\|_{L^2(0,t_n;H^{-1}(\Omega))}^2. \end{aligned}$$

By the estimate (4.8), we obtain

$$\sum_{p=1}^{n}(\eta_t^p)^2 \lesssim E(t_n)^2 + \|f-\pi_\tau f\|^2_{L^2(0,t_n;H^{-1}(\Omega))}. \tag{6.4}$$

On the other hand, by Corollary 5.7, we have

$$\sum_{p=1}^{n}\tau_p(\eta^p)^2 \lesssim \int_0^{t_n}\|\partial_t(u_\tau-u_{h\tau})(t)\|^2_{1,\omega_K}\,dt + \sum_{p=1}^{n}\tau_p\|e^p\|^2_{a_1} + \sum_{p=1}^{n}\tau_p(\xi_K^p)^2.$$

Again thanks to (4.8), we obtain

$$\sum_{p=1}^{n}\tau_p(\eta^p)^2 \lesssim E(t_n)^2 + \sum_{p=1}^{n}\tau_p(\xi^p)^2. \tag{6.5}$$

The estimate (6.2) directly follows from (6.4) and (6.5). □

Remark 6.2. — Under Assumptions 5.4 and 5.5, Theorem 6.1 states that the error $E(t_n)$ is equivalent to the global error estimator

$$\left(\sum_{p=1}^{n}\left((\eta_t^p)^2+\tau_p(\eta^p)^2\right)\right)^{1/2},$$

up to approximation terms. Since each term of this global error estimator is computable, it may be used for an adaptive algorithm.

7. Numerical experiments

Our theoretical analysis is now confirmed by different numerical examples. The first two ones are used to confirm the efficiency and reliability of our error estimator, while the third and fourth ones illustrate the usefulness of our estimator by presenting an adaptive algorithm for solutions having a singular behaviour in space. For simplicity all the tests will be performed with $L_1 = I-\Delta$ and $L_2 = -\Delta$ (Δ being the standard Laplace operator).

7.1. **A validation test.** This example consists in solving the two dimensional Sobolev equation on the unit square $\Omega =]0,1[\times]0,1[$. Here, we use the Lagrange element on a regular mesh $T_{ph} = T_h$ obtained by dividing each segment by n subintervals and dividing each obtained square into two triangles (see Figure 7.1).

The tests are performed with $T = 1s$ and the following exact solution

$$u(x,y,t) = e^{-t}xy(x-1)(y-1) \text{ in } \Omega\times]0,1[,$$

so that $u_0(x,y) = xy(x-1)(y-1)$ in Ω and $u(.,t)_{|\Gamma} = 0$, for all $t \in]0,1[$. All numerical results will be presented at the final time $T = 1s$.

First, we check that the numerical solution u_h^N converges towards the exact one. For that purpose, we have plotted in Figure 7.2 the error $|u(\cdot,t_N) - u_h^N|^2_{1,\Omega}$ as a function of the meshsize (resp. time step) when the time step (resp. meshsize) is fixed and small enough. Here and below a double logarithmic scale is used in such a way that the slope of the curves gives the order of convergence. As we can see, this figure underlines the theoretical predicted optimal order of convergence h (resp. τ_p) as τ_p (resp. h) is fixed and small enough (see [3]).

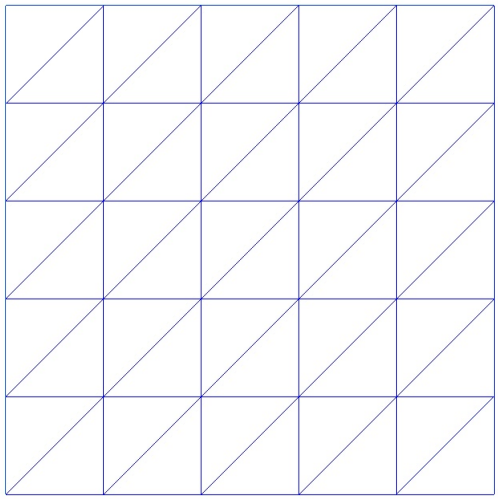

FIGURE 7.1. The mesh on the unit square with $h = 0.2$.

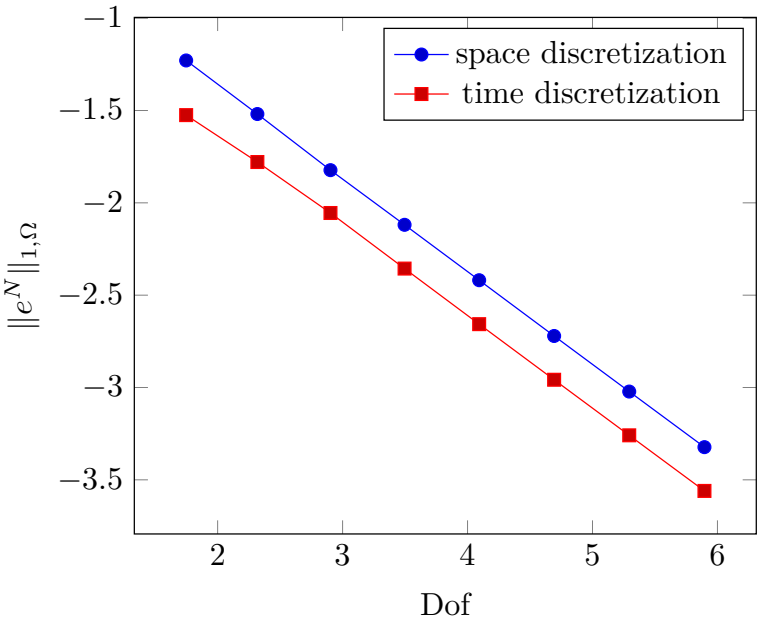

FIGURE 7.2. $\|u(\cdot, t_N) - u_h^N\|_{1,\Omega}$ as a function of Dof at final time $T = 1s$ for different h with $\tau_p = 0.001s$ (resp. τ_p with $h = 0.00625$).

Now we investigate the main theoretical results which are the upper and lower error bounds (5.2) and (5.7). For that purpose, we fix a small time step $\tau_p = 0.1s$ and let vary the meshsize h.

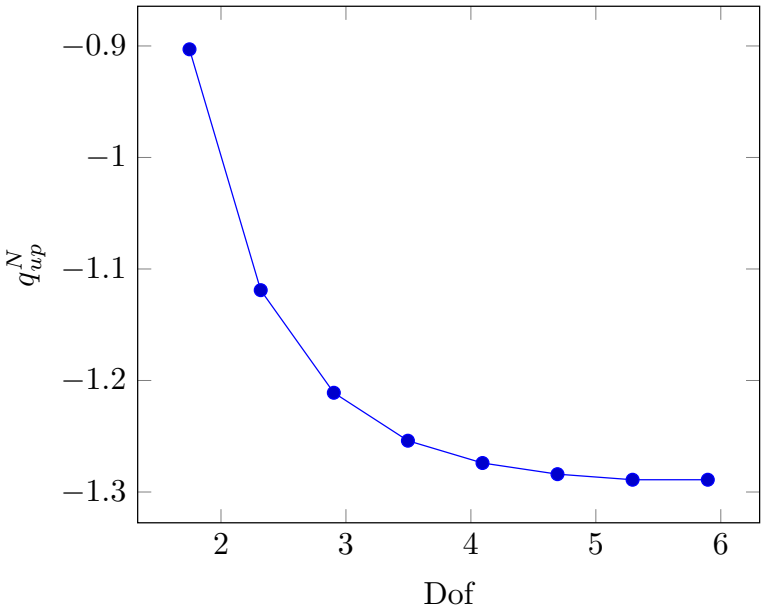

FIGURE 7.3. q_{up}^N wrt DoF for uniform meshes

7.1.1. *Reliability of the spatial estimator.* First, we define the ratio of the left-hand side and the right-hand side of the estimate (5.2) at the last time $T = 1s$:

$$q_{up}^N = \frac{\|e^N\|_{1,\Omega}^2 + \sum_{p=1}^{N} \tau_p |e^p|_{1,\Omega}^2}{\|e^0\|_{1,\Omega}^2 + \sum_{p=1}^{N} \tau_p \sum_{K \in T_{ph}} ((\eta_K^p)^2 + h_K^2 \|f^p - f_h^p\|_K^2)}.$$

q_{up}^N is referred as the *effectivity index*. It measures the *reliability* of the estimator and is related to the global upper error bound. From Theorem 5.2, the ratio q_{up}^N is bounded from above. This is confirmed by our numerical results presented in Figure 7.3 and Table 7.1. Hence, the spatial estimator is reliable.

7.1.2. *Efficiency of the spatial estimator.* Now, we define the (larger) ratio of the left-hand side and the right-hand side of the estimate (5.7) at the final time $T = 1s$:

$$q_{low}^N = \max_{K \in T_{ph}} \frac{\eta_K^N}{h_K \| \frac{e^N - e^{N-1}}{\tau_p} \|_{1,\omega_K} + \|e^N\|_{1,\omega_K} + h_K \|f^N - f_h^N\|_{\omega_K}}.$$

q_{low}^N is related to the local lower error bound and measures the *efficiency* of the estimator. According to Figure 7.4 (see also Table 7.1), q_{low}^N is bounded from above as theoreticaly predicted in Theorem 5.6. Therefore our spatial estimator is also efficient.

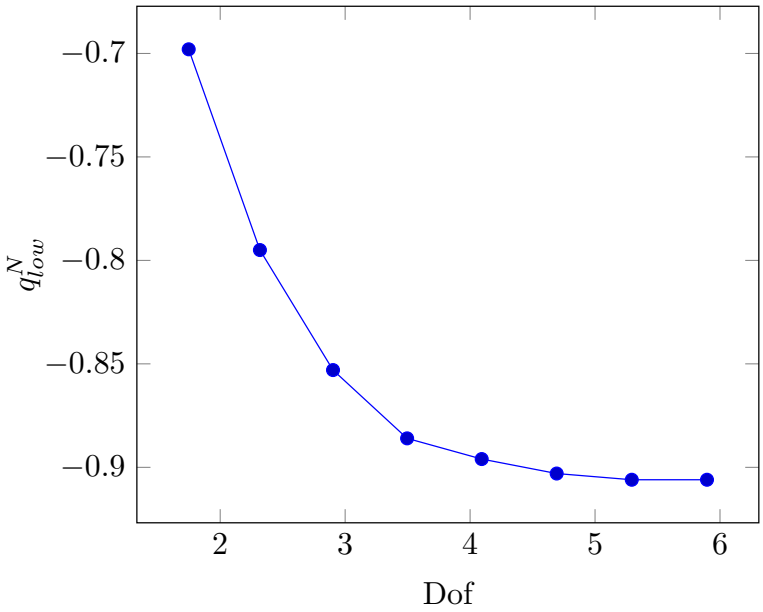

FIGURE 7.4. q^N_{low} wrt DoF for uniform meshes

n	DoF	q^N_{up}	q^N_{low}
4	56	0.125	0.20
8	208	0.0759	0.16
16	800	0.0614	0.14
32	3136	0.0557	0.13
64	12416	0.0532	0.127
128	49408	0.0519	0.125
256	197120	0.0514	0.124
512	787456	0.0513	0.123

TABLE 7.1. q^N_{up} and q^N_{low} wrt DoF for uniform meshes.

7.1.3. *Non structured meshes.* In order to validate the reliability and efficiency of our spatial error estimator, we have approximated the same problem as before with the same elements but on different non structured meshes obtained by starting from a rough non structured mesh of size 0.2 (see Figure 7.5) and by dividing each triangle into 4 triangles by the standard regular refinements [27]. Figures 7.6 and 7.7 (see also Table 7.2) show respectively the rations q^N_{up} and q^N_{low} with respect to the degrees of freedom. Again we may conclude that both ratios are bounded from above and consequently our spatial error estimator is reliable and efficient.

7.2. **Dependence of the error.** From our previous considerations, the error between the exact solution and its approximated one is expected to depend on the

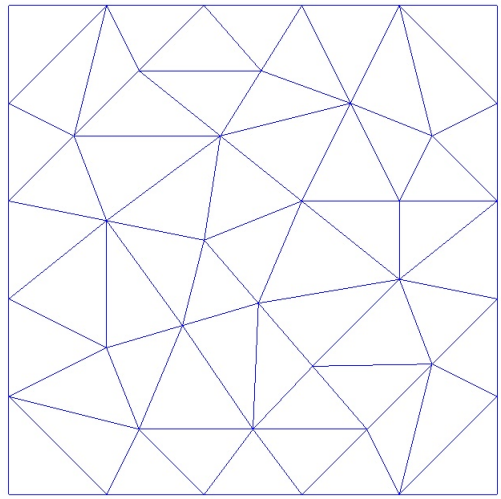

FIGURE 7.5. The non structured mesh on the unit square with $h = 0.2$.

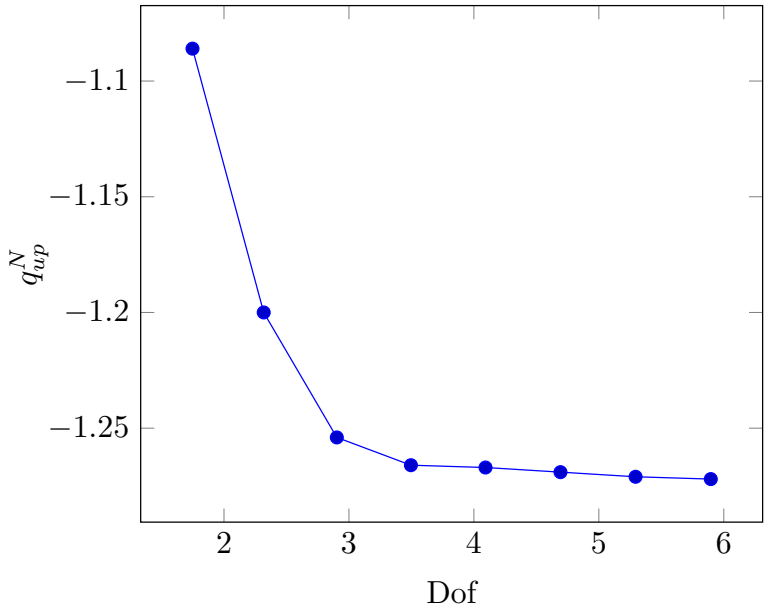

FIGURE 7.6. q_{up}^N wrt DoF for non structured meshes

space and/or time discretization. In order to illustrate this phenomenon, as in [18, 21], we exhibit an example where the error due to the time discretization is more important than the error due to the space discretization, and another example where the converse phenomenon appears. For that purpose we consider the

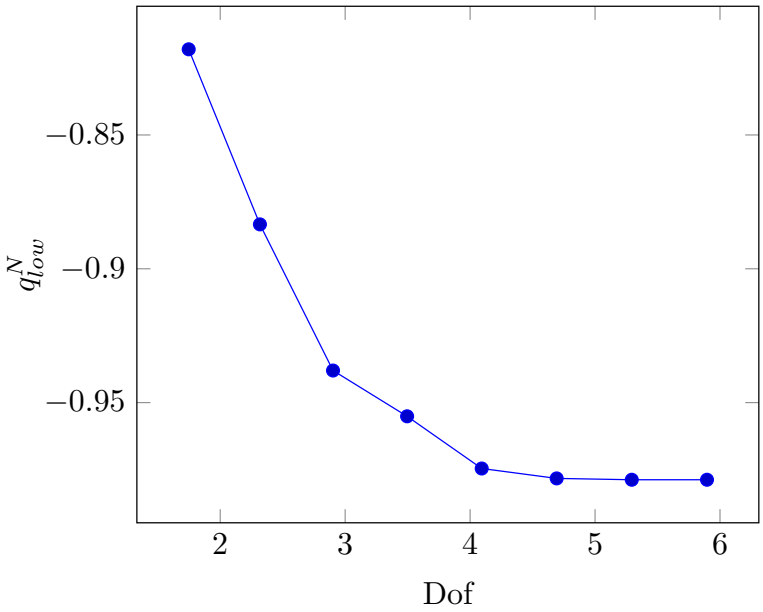

FIGURE 7.7. q^N_{low} wrt DoF for non structured meshes

n	DoF	q^N_{up}	q^N_{low}
4	56	0.0819	0.1525
8	208	0.0630	0.13077
16	800	0.0556	0.1153
32	3136	0.0542	0.10899
64	12416	0.05398	0.1060
128	49408	0.05387	0.1051
256	197120	0.0534	0.105

TABLE 7.2. q^N_{up} and q^N_{low} wrt DoF for non structured meshes.

problem (2.3) for $\Omega =]0,1[\times]0,1[$ and $T = 1s$, with the exact solution u_1 and u_2 defined by:

$$u_1 = \sin(\pi x)\sin(\pi y)\sin(\pi t),$$
$$u_2 = \sin(\pi x)\sin(\pi y)\sin t.$$

The numerical results are shown in Tables 7.3 and 7.4, where we present the values of the space indicator η, the time indicator η_t, the error $\|e\| := \max_{1\leqslant p\leqslant N} \|e^p\|_{1,\Omega}$ and the spatial effectivity index q^N_{up} for different uniform triangulations and constant time steps. In the first case, we can conclude that the error is mainly due to the time discretization. Indeed from Table 7.3, we see that for a fixed time step and decreasing mesh sizes, the error is almost constant, while for a fixed mesh size and decreasing time steps, the error decreases. We moreover remark a close relationship

between the error and the time indicator. For the second example, the error is mainly due to the time discretization, since we see converse relations between the error and the time steps and mesh size, while we clearly detect a relationship between the error and space indicator. For the first example q_{up}^N is correlated to the error, while for the second one, the distortion comes for the approximation terms. Let us further remark that the numerical experiments bring to light that the indicator η_t is independent of h, while the indicator η is mainly independent of τ_p. This important property of uncoupling the two error parts is effectively used in our adaptive algorithm described below, since the time (resp. space) refinements or unrefinements are (mainly) based on η_t (resp. η).

$h = 1/n$	0.1	0.05	0.025	0.0125	0.1	0.05	0.025	0.0125
dt	0.1	0.1	0.1	0.1	0.05	0.05	0.05	0.05
η	4.62	2.32	1.16	0.58	4.34	2.16	1.08	0.54
η_t	0.22	0.22	0.22	0.22	0.077	0.077	0.077	0.077
$\|e\|$	0.53	0.53	0.53	0.53	0.265	0.265	0.265	0.265
q_{up}^N	1.77e-4	1.5e-4	1.5e-4	1.5e-4	4.77e-5	4.25e-5	4.25e-5	4.77e-5
$h = 1/n$	0.1	0.05	0.025	0.0125	0.1	0.05	0.025	0.0125
dt	0.025	0.025	0.025	0.025	0.0125	0.0125	0.0125	0.0125
η	4.48	2.24	1.12	0.56	4.60	2.30	1.15	0.57
η_t	0.027	0.027	0.027	0.027	0.009	0.009	0.009	0.009
$\|e\|$	0.13	0.13	0.13	0.13	0.06	0.06	0.06	0.06
q_{up}^N	1.57e-5	1.46e-5	1.02e-5	1.01e-5	3.70e-6	3.60e-006	3.54e-6	3.50e-6

TABLE 7.3. Convergence results when using uniform triangulations and constant time steps for the first example.

$h = 1/n$	0.1	0.05	0.025	0.0125	0.1	0.05	0.025	0.0125
dt	0.1	0.1	0.1	0.1	0.05	0.05	0.05	0.05
η	2.56	1.29	0.65	0.32	2.52	1.27	0.65	0.32
η_t	0.039	0.039	0.039	0.039	0.014	0.014	0.014	0.014
$\|e\|$	0.30	0.16	0.08	0.04	0.30	0.16	0.08	0.04
q_{up}^N	1.36e-4	4.13e-5	2e-5	1.18e-5	1.36e-4	4.13e-5	2e-5	1.18e-5
$h = 1/n$	0.1	0.05	0.025	0.0125	0.1	0.05	0.025	0.0125
dt	0.025	0.025	0.025	0.025	0.0125	0.0125	0.0125	0.0125
η	2.52	1.27	0.64	0.32	2.52	1.27	0.64	0.32
η_t	0.0049	0.0049	0.0049	0.0049	0.0017	0.0017	0.0017	0.0017
$\|e\|$	0.30	0.16	0.08	0.04	0.30	0.16	0.08	0.04
q_{up}^N	1.36e-4	4.13e-5	2e-5	1.18e-5	1.36e-4	4.13e-5	2e-5	1.18e-5

TABLE 7.4. Convergence results when using uniform triangulations and constant time steps for the second example.

7.3. **An adaptive algorithm.** From our theoretical considerations and the examples of the previous subsection, an adaptive algorithm has to use appropriately the space indicator η, the time indicator η_t and the approximation error ξ. To design this algorithm, we first define the global indicator $\bar{\eta}$ as follows

$$\bar{\eta} := \left(\sum_{n=1}^{N} ((\eta_t^n)^2 + \tau_n(\eta^n)^2 + \tau_n(\xi^n)^2) \right)^{1/2}.$$

For our approximated solution $u_{h\tau}$, we define a relative error estimator **Ind** by

$$\mathbf{Ind}^2 = \frac{\bar{\eta}^2}{\int_0^T \|\nabla u_{h\tau}\|^2 dt}. \tag{7.1}$$

Let a preset tolerance δ and a parameter $0 \leqslant \alpha \leqslant 1$ be given. The goal of our adaptive scheme is to generate a sequence of sub-intervals $[t_{n-1}, t_n]$ and mesh triangulations $T_{nh}, n = 1, ..., N$ such that Ind, defined by (7.1), is close to the preset of tolerance δ, in the sense that

$$(1-\alpha)\delta \leqslant \mathbf{Ind} \leqslant (1+\alpha)\delta. \tag{7.2}$$

To achieve these bounds, for all $n = 1, ..., N$, we define two local bounds: a left one $\mathbf{Lb}^n$ defined by

$$\mathbf{Lb}^n := (1-\alpha)^2\delta^2 \int_{t_{n-1}}^{t_n} \|\nabla u_{h\tau}(\cdot, t)\|^2 dt, \tag{7.3}$$

and a right one $\mathbf{Rb}^n$ defined by

$$\mathbf{Rb}^n := (1+\alpha)^2\delta^2 \int_{t_{n-1}}^{t_n} \|\nabla u_{h\tau}(\cdot, t)\|^2 dt. \tag{7.4}$$

If, for all $n = 1, ..., N$, the conditions

$$\mathbf{Lb}^n \leqslant (\eta_t^n)^2 + \tau_n(\eta^n)^2 + \tau_n(\xi^n)^2 \leqslant \mathbf{Rb}^n \tag{7.5}$$

are satisfied, then summing from $n = 1$ to $n = N$, we obtain (7.2). Thus our algorithm, described in Algorithm 1, consists in finding time steps and triangulations such that (7.5) holds for all n. This will be achieved by using the elements η^n and ξ^n to control the mesh sizes, and using ξ^n and η_t^n to control the time steps. Note that it is similar to the one proposed in [18, 21].

In order to test our adaptive scheme, we consider two relevant examples. The first one when the Sobolev equation (2.3) is considered in the unit square $]0, 1[\times]0, 1[$ with the exact solution defined by (see [18, 21])

$$u(x, y, t) = \beta(t) * \exp(-50 * r^2(x, y, t)), \tag{7.6}$$

with $r^2(x, y, t) = (x - 0.4 * t - 0.3)^2 + (y - 0.4 * t - 0.3)^2$, and

$$\beta(t) = \begin{cases} 1 - \exp(-50 * (0.98 * t + 0.01)^2) & \text{if } t < 1/1.96, \\ 1 - \exp(-50 * (1 - 0.98 * t + 0.01)^2) & \text{else .} \end{cases} \tag{7.7}$$

This means that u is a Gaussian function whose center moves from point $(0.3, 0.3)$ at time $t = 0s$ to point $(0.7, 0.7)$ at time $t = 1s$. The obtained meshes at times $0.1, 0.5$ and 1 are shown in Figures 7.8 with the tolerance $\delta = 0.25$ and the parameter $\alpha = 0.5$. From these figures we may conclude that the meshes are refined in the

region of a large gradient of the solution and then follow correctly the moving centers.

Algorithm 1 The adaptive algorithm

```
Set T_0h, n = 1, t, τ                                  Initialization
while t ⩽ T do
  Compute (η^n)^2, (η_t^n)^2,
  (ξ^n)^2, Rb^n, Lb^n
  if (τ_n ξ^n/2 + η_t^n) < Lb^n then
                                                       Current time step is to small
    τ := 2τ                                            Same time iteration with bigger step
  else if (τ_n (ξ^n)^2/2 + (η_t^n))^2 ⩽ Rb^n then
    if τ_n((η^n)^2 + (ξ^n)^2/2) < Lb^n then
      Continue with criteria                           Triangulation is too fine
      η_K^n ⩽ 1.5 min η_K^n
    else if τ_n((η^n)^2 + (ξ^n)^2/2) < Rb^n then
                                                       Mesh Triangulation is correct
      t := t+τ                                         Incrementation of the current time step

      n := n + 1
    else
      Continue with criteria                           Mesh Triangulation is too coarse
      η_K^n ⩾ 0.5 min η_K^n                            Same time with finer triangulation
    end if
  else
    Time step is too large
    τ := τ/2                                           Same time iteration with smaller time
                                                       step
  end if
  Generate the new triangulation
end while
```

As second example, we consider the Sobolev equation (2.3) in the L-shaped domain $]-1,1[^2\backslash(]0,1[\times]0,-1[)$ with exact solution defined by

$$u(r,\theta) = e^{-t} * r^{2/3}\sin\left(\frac{2}{3}\theta\right),$$

where (r,θ) are polar coordinates centred at $(0,0)$. In that case, u has a singular behaviour along the edge $(0,0)\times]0,T[$. This behavior induces a refinement of the mesh near $(0,0)$ during the adaptive algorithm, as Figure 7.9 shows for $t = 0.1$. We do not present the meshes for the other time steps since they have a very similar form as the one for $t = 0.1$.

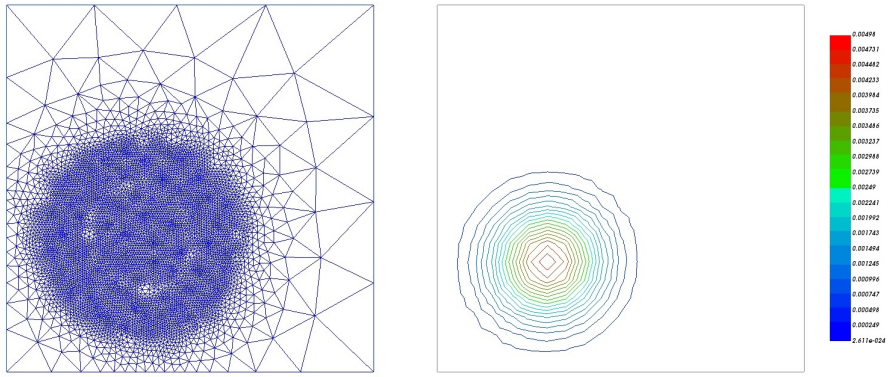

$n = 4,\ t_n = 0.1s, Nv = 441$

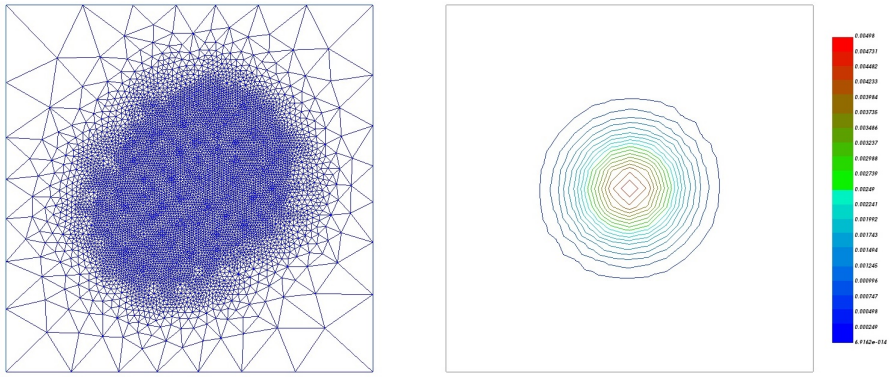

$n = 4,\ t_n = 0.5s, Nv = 441$

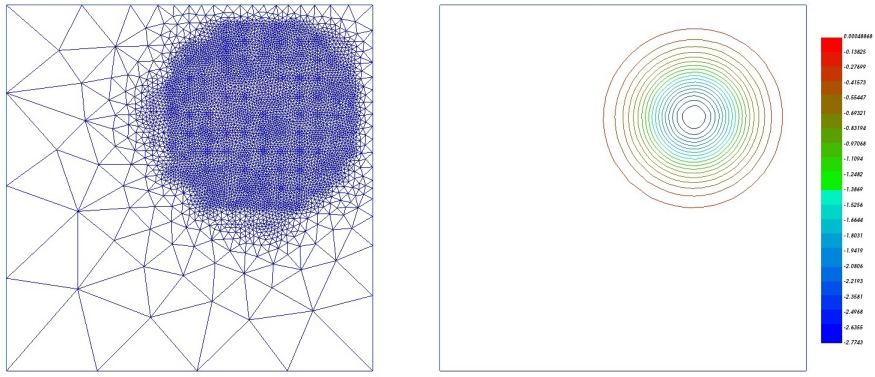

$n = 4,\ t_n = 1s, Nv = 441$

FIGURE 7.8. Adapted triangulations and isovalues of $u_{h\tau}$ at time 0.1, 0.5, 1 ($\delta = 0.25,\ \alpha = 0.5$).

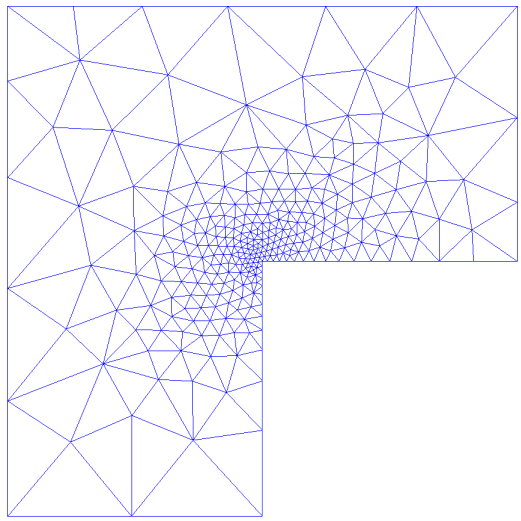

FIGURE 7.9. Adapted triangulation at time $t = 0,1$ with $\alpha = 0.5$ and $\delta = 0.25$.

REFERENCES

[1] D. N. Arnold, J. Douglas, Jr., and V. Thomée. Superconvergence of a finite element approximation to the solution of a Sobolev equation in a single space variable. *Math. Comp.*, 36(153):53–63, 1981.

[2] G. I. Barenblatt, V. M. Entov, and V. M. Ryzhik. *Theory of fluid flow through natural rocks*. Dordrecht: Kluwer, 1990.

[3] F. Bekkouche, W. Chikouche, and S. Nicaise. Fully discrete approximation of general nonlinear Sobolev equations. *Afr. Mat.*, Sep 2018.

[4] A. Bergam, C. Bernardi, and Z. Mghazli. A posteriori analysis of the finite element discretization of some parabolic equations. *Math. Comp.*, 74(251):1117–1138, 2005.

[5] C. Bernardi and B. Métivet. Indicateurs d'erreur pour l'équation de la chaleur. *Revue Européenne des éléments finis*, 9(4):425–438, 2000.

[6] C. Bernardi and R. Verfürth. A posteriori error analysis of the fully discretized time-dependent Stokes equations. *M2AN Math. Model. Numer. Anal.*, 38(3):437–455, 2004.

[7] J. M. Cascón, L. Ferragut, and M. I. Asensio. Space-time adaptive algorithm for the mixed parabolic problem. *Numer. Math.*, 103(3):367–392, 2006.

[8] P. J. Chen and M. E. Gurtin. On a theory of heat conduction involving two temperatures. *Z. Angew. Math. Phys.*, 19:614–627, 1968.

[9] P. Ciarlet. The finite element method for elliptic problems. *North Holland*, 1996.

[10] P. Clément. Approximation by finite element functions using local regularization. *Rev. Française Automat. Informat. Recherche Opérationnelle Sér.*, 9(R-2):77–84, 1975.

[11] B. D. Coleman and W. Noll. An approximation theorem for functionals, with applications in continuum mechanics. *Arch. Rational Mech. Anal.*, 6:355–370 (1960), 1960.

[12] C. Cuesta, C. J. van Duijn, and J. Hulshof. Infiltration in porous media with dynamic capillary pressure: travelling waves. *European J. Appl. Math.*, 11(4):381–397, 2000.

[13] R. E. Ewing. Time-stepping Galerkin methods for nonlinear Sobolev partial differential equations. *SIAM J. Numer. Anal.*, 15(6):1125–1150, 1978.

[14] S. M. Hassanizadeh and W. G. Gray. Thermodynamic basis of capillary pressure in porous media. *Water Resour. Res.*, 29:858–879, 1993.

[15] P. Houston and E. Süli. Adaptive Lagrange-Galerkin methods for unsteady convection-diffusion problems. *Math. Comp.*, 70(233):77–106, 2001.

[16] C. Johnson, Y. Y. Nie, and V. Thomée. An a posteriori error estimate and adaptive timestep control for a backward Euler discretization of a parabolic problem. *SIAM J. Numer. Anal.*, 27(2):277–291, 1990.
[17] T. Liu, Y.-p. Lin, M. Rao, and J. R. Cannon. Finite element methods for Sobolev equations. *J. Comput. Math.*, 20(6):627–642, 2002.
[18] S. Nicaise and N. Soualem. A posteriori error estimates for a nonconforming finite element discretization of the heat equation. *M2AN Math. Model. Numer. Anal.*, 39(2):319–348, 2005.
[19] M. R. Ohm and H. Y. Lee. L^2-error analysis of fully discrete discontinuous Galerkin approximations for nonlinear Sobolev equations. *Bull. Korean Math. Soc.*, 48(5):897–915, 2011.
[20] M. R. Ohm, H. Y. Lee, and J. Y. Shin. L^2-error estimates of the extrapolated Crank-Nicolson discontinuous Galerkin approximations for nonlinear Sobolev equations. *J. Inequal. Appl.*, pages Art. ID 895187, 17, 2010.
[21] M. Picasso. Adaptive finite elements for a linear parabolic problem. *Comput. Methods Appl. Mech. Engrg.*, 167(3-4):223–237, 1998.
[22] M. Picasso. An anisotropic error indicator based on Zienkiewicz-Zhu error estimator: Application to elliptic and parabolic problems. *SIAM J. Sci. Comput.*, 24(4):1328–1355, 2003.
[23] R. E. Showalter. The Sobolev equation. II. *Applicable Anal.*, 5(2):81–99, 1975.
[24] T. W. Ting. Certain non-steady flows of second-order fluids. *Arch. Rational Mech. Anal.*, 14:1–26, 1963.
[25] T. W. Ting. A cooling process according to two-temperature theory of heat conduction. *J. Math. Anal. Appl.*, 45:23–31, 1974.
[26] T. Tran and T.-B. Duong. A posteriori error estimates with the finite element method of lines for a Sobolev equation. *Numer. Methods Partial Differential Equations*, 21(3):521–535, 2005.
[27] R. Verfürth. A review of a posteriori error estimation and adaptive mesh-refinement techniques. *Wiley-Teubner, Chichester; Stuttgart*, 1996.
[28] R. Verfürth. Error estimates for some quasi-interpolation operators. *M2AN Math. Model. Numer. Anal.*, 33(4):695–713, 1999.
[29] R. Verfürth. A posteriori error estimates for finite element discretization of the heat equation. *Calcolo*, 40:195–212, 2003.

Manuscript received May 22, 2018,
revised January 14, 2019,
accepted May 29, 2019.

Serge NICAISE & Fatiha BEKKOUCHE
Univ. Polytechnique Hauts-de-France, EA 4015 LAMAV, FR CNRS 2956, F-59313 Valenciennes, France
Serge.Nicaise@uphf.fr (Corresponding author)
f_bekkouche@yahoo.fr